Escherichia coli Purine Repressor: Key Residues for the Allosteric Transition between Active and Inactive Conformations and for Interdomain Signaling[†]

Fu Lu,[‡] Richard G. Brennan,[§] and Howard Zalkin*,[‡]

Department of Biochemistry, Purdue University, West Lafayette, Indiana 47907-1153, and Department of Biochemistry and Molecular Biology, Oregon Health Sciences University, Portland, Oregon 97201-3098

Received July 7, 1998; Revised Manuscript Received August 24, 1998

ABSTRACT: The *Escherichia coli* purine repressor, PurR, exists in an equilibrium between open and closed conformations. Binding of a corepressor, hypoxanthine or guanine, shifts the allosteric equilibrium in favor of the closed conformation and increases the operator DNA binding affinity by 40-fold compared to aporepressor. Glu70 and Trp147 PurR mutations were isolated which perturb the allosteric equilibrium. Three lines of evidence indicate that the allosteric equilibrium of E70A and W147A aporepressors was shifted toward the closed conformation. First, compared to wild-type PurR, these mutant repressors had a 10−30-fold higher corepressor binding affinity. Second, the mutant aporepressors bound to operator DNA with an affinity that is characteristic of the wild-type PurR holorepressor. Third, binding of guanine to wild-type PurR resulted in a near-UV circular dichroism spectral change at 297−305 nm that is attributed to the closed conformation. The circular dichroism spectrum of the E70A aporepressor at 297−305 nm was that expected for the closed conformation, and it was not appreciably altered by corepressor binding. Mutational analysis was used to identify an Arg115−Ser46′ interdomain intersubunit hydrogen bond that is necessary for transmitting the allosteric transition in the corepressor binding domain to the DNA binding domain. R115A and S46G PurR mutants were defective in DNA binding in vitro and repressor function in vivo although corepressor binding was identical to the wild type. These results establish that the hydrogen bond between the side chain NH_2 of Arg115 and the main chain CO of Ser46′ plays a critical role in interdomain signaling.

Escherichia coli purine repressor (PurR)[1] regulates the transcription of the genes required for de novo purine biosynthesis and several genes for related pathways (*1*). PurR is a 76 kDa homodimer. Each subunit is composed of an NH_2-terminal DNA binding domain connected by a hinge sequence to a larger corepressor binding and dimerization domain (CBD) (*2*, *3*). The hinge itself is also important for DNA binding (*4*). The DNA binding affinity is modulated by guanine and hypoxanthine corepressors (*5*) that bind in the cleft between NH_2- and COOH-subdomains of the CBD (*6*). PurR is a member of the large LacI repressor family, all members of which are regulated by small-molecule effectors that act either as inducers or as corepressors (*7*, *8*).

The molecular basis for the corepressor-modulated DNA binding remained unknown until X-ray structures of the ternary PurR−corepressor−DNA complex (*6*) and a corepressor-free CBD dimer (*9*) were determined. This work led to a structure-based mechanism for corepressor-mediated specific DNA binding. The structures establish that PurR exists in corepressor-free "open" and corepressor-bound "closed" conformations. The CBD structural change is localized to the NH_2-terminal subdomain whereas the COOH-terminal subdomain does not change. When a corepressor binds to the CBD, the two NH_2-subdomains rotate by about 20°, whereas the COOH-subdomains remain fixed. Consequently, Lys60, the NH_2-terminal residue of the CBD, moves 3.5 Å closer to Lys60′ in the other subunit. This structure change in CBD is propagated to the hinge helix and the helix−turn−helix motif in the DNA binding domain. In fact, the hinge regions of the monomers are brought into apposition and pack against each other by van der Waals contacts. In the presence of a specific DNA site, local folding of the hinge helices can take place accompanied by specific interaction with the DNA minor groove. The resultant DNA kinking permits the 2-fold related helix−turn−helix motifs to make appropriate contacts with the consecutive major groove base pairs of the operator site (*6*). As a result of the open to closed conformational transition, the DNA binding affinity of PurR is significantly increased, and transcription of the *pur* regulon genes is down-regulated.

The PurR X-ray structures describe two static allosteric states. Although they serve as a good starting point to understand the allosteric transition mechanism, further investigation is necessary in order to assess the role played by specific residues in the stabilization of either the open or the closed states and to identify the pathways by which corepressor-mediated CBD changes are coupled to the DNA binding domain. We have used site-directed mutagenesis to address these issues.

[†] Supported by U.S. Public Health Service Grants GM24658 (H.Z.) and GM49244 (R.G.B.). This is journal paper 15790 from the Purdue University Agricultural Research Station.

* Corresponding author. Phone: 765-494-1618. Fax: 765-494-7897. E-mail: zalkin@biochem.purdue.edu.

[‡] Purdue University.

[§] Oregon Health Sciences University.

[1] Abbreviations: PurR, purine repressor; CBD, corepressor binding domain; CD, circular dichroism; Gua, guanine; Hyp, hypoxanthine.

10.1021/bi981617k CCC: $15.00
Published on Web 10/22/1998

It has been documented for well-characterized allosteric proteins such as hemoglobin (*10*), aspartate transcarbamoylase (*11*, *12*), and phosphofructokinase (*13*), that key interactions between residues in different domains or different subunits are likely to play an important role in the allosteric transition. To dissect the PurR allosteric transition mechanism in molecular detail, functional residues were inferred by comparison of the liganded and unliganded PurR structures. A complex rearrangement takes place in the CBD NH_2-subdomain interface and the corepressor binding pocket upon corepressor binding. Residues Glu70 and Trp147 were recognized to have different interactions in the open and closed conformations (*6*, *9*). In the closed conformation, Glu70 forms an intersubunit salt bridge with Arg278′ that links the NH_2-subdomain of one subunit to the COOH-subdomain of the other subunit. In the open structure, this salt bridge does not exist. Rather, Glu70 and its dimer mate are close to a Mg^{2+} that is located at the 2-fold symmetry axis between the two NH_2-subdomains (PDB code 1DBQ). Glu70 and Glu70′ may form an ionic bridge with Mg^{2+}. Trp147 is not involved in intersubunit interaction. It was identified as a key switch residue in the corepressor binding pocket (*6*). In the holorepressor, Trp147 is far removed from the corepressor binding pocket and stacks against Tyr126. However, in the open state, it rotates into the ligand binding pocket, resulting in a 10.7 Å translation of its Nϵ atom. In this position, Trp147 hydrogen bonds to the side chain of Tyr73 by its Nϵ and stacks against Phe74. Thus, it appears that Trp147 may play a role as the structural surrogate of corepressor to stabilize the open conformation (*6*, *9*).

To date, corepressor-mediated specific DNA binding has been characterized structurally for only *E. coli* TrpR (*14*) and MetJ (*15*, *16*) repressors. However, unlike TrpR and MetJ where corepressor binds at the same domain used for DNA binding, in PurR corepressor binds to a separate domain, the CBD, at a distance of more than 40 Å from the DNA binding domain (*6*). The signal of corepressor binding needs to be transmitted from the CBD to the DNA binding domain in order to increase DNA binding affinity. In the PurR−hypoxanthine−*purF* complex, there are three hydrogen bonds between the DNA binding domain of one subunit and the CBD of the other, formed between the NH1 and NH2 of Arg115 with side-chain and main-chain CO, respectively, of Ser46′, and the main-chain carbonyl oxygen of Gln113 with the backbone NH of Ala49′. However, in the unliganded structure, the helical hinge region is disordered (*17*), rendering motions of the DNA binding domain essentially independent of the CBD. Consequently, the hydrogen bonds that connect the DNA binding domain to the CBD no longer exist. It was suspected that these hydrogen bond interactions may play a role in coupling the conformational change between the CBD and the DNA binding domain.

To probe the function of Trp147, Glu70, and Arg278 in the CBD allosteric transition, we have used site-directed mutagenesis to replace these residues. To investigate the role of hydrogen bonds in interdomain signaling between subunits, mutations to residues Arg115, Ser46, Gln113, and Ala49 were designed to break the hydrogen bonds. We report here a biochemical and biophysical analysis of the mutant repressors and evaluate the roles of these residues in the allosteric transition mechanism.

MATERIALS AND METHODS

Site-Directed Mutagenesis. All mutant genes were constructed using the method of Kunkel et al. (*18*). Oligonucleotides, synthesized in the Purdue University Laboratory for Macromolecular Structure, were purified using a Sephadex-G25 gel filtration column.

Expression and Purification of Native and Mutant Apo-PurR Proteins. All the PurR proteins were produced and purified according to the methods described previously (*19*) except that purified proteins were concentrated at room temperature instead of at 4 °C. Higher temperature increases the solubility of PurR protein (R. G. Brennan, unpublished). The protein concentration was determined by the Lowry method (*20*).

For E70A, W147A, and W147A/R190A superrepressor proteins, corepressor was not removed from PurR by the above purification procedure as determined by X-ray crystallography (J. L. Huffman and R. G. Brennan, unpublished). Aporepressor proteins were obtained from the holorepressors by a partial denaturation, column separation, and renaturation process. Holosuperrepressors were treated with 1 M guanidine hydrochloride in 10 mM Tris, pH 8.0, for 1 h. The apoprotein and corepressor were separated by gel filtration through a Sephadex G50 column (0.7 × 10 cm) in 1 M guanidine hydrochloride/10 mM Tris, pH 8.0. Fractions containing the apoprotein were pooled, and PurR was renatured by dialysis for 2 h in buffer A (10 mM Hepes, pH 7.6, 5% glycerol, 0.2 mM DTT, 0.1 mM EDTA) containing 160 mM potassium phosphate. To monitor the separation process, the bound corepressor was first exchanged with [^{14}C]-guanine by overnight incubation with excess [^{14}C]guanine in a 5:1 molar ratio ([^{14}C]guanine:protein monomer ratio). The successful removal of corepressor following the column process was verified by measuring the removal of radioactivity in the fractions containing protein. The efficiency of the [^{14}C]guanine exchange reaction was determined by a control experiment in which the protein was not treated with guanidine hydrochloride.

Assay for in Vivo Function. The in vivo function of wild-type and mutant PurR was assayed using a system in which the *purR* gene was incorporated into the chromosome in single copy and repressor function was monitored by the expression level of a *purF-lacZ* reporter (*19*, *21*). Briefly, wild-type and mutant *purR* genes were cloned into the conditionally replicative, integrative plasmid pCAH63. The resulting plasmid, pCAH64-*purR*, was integrated into the chromosome of strain FL100 (*purR*$^-$, *purF-lacZ*) carrying pINT-*ts* that provides integration function. Finally, the single-copy integrants were verified by PCR testing as described (*19*). The β-galactosidase assays were performed as described previously (*21*) according to the method of Miller (*22*). For strains with *purR* superrepressor genes, the β-galactosidase reporter was repressed to very low levels. It was therefore necessary to extend the incubation time to 15 h in order to develop measurable product.

Alternatively, the in vivo function of superrepressors was tested for their capacity to inhibit cell growth in minimal medium (*2*) without a purine supplement. Wild-type, E70A, W147A, and W147A/R190A *purR* genes were integrated into the chromosome of strain R220 (*purR*$^-$) (*23*) using the same procedure described above. To obtain the growth curve, 1

mL of fresh overnight culture from a single colony was used to inoculate 50 mL of minimal medium (*2*) in a 250 mL sidearm flask. The cells were grown with shaking at 37 °C, and cell density was recorded at 1 h intervals using a Klett colorimeter. Doubling time in the log growth phase for each strain was determined from the growth curve.

Corepressor Binding. Equilibrium dialysis was used to determine the binding affinity of corepressor (*3*, *19*). Buffer system II (100 mM Hepes, pH 7.5, 250 mM potassium glutamate, 50 mM NaCl, 10 mM magnesium acetate, 1 mM EDTA, 2% dimethyl sulfoxide) was employed for the binding measurements. Binding data were fit to eq 1 using Ultrafit software (Biosoft, Cambridge, U.K.) (*3*). *Y* is fractional saturation; K_d, the dissociation constant; L, free corepressor; and *n*, the Hill coefficient.

$$Y = [L]^n/(K_d n + [L]^n) \quad (1)$$

DNA Binding. Operator DNA binding in the presence or absence of 200 μM hypoxanthine corepressor was measured by gel retardation assay (*5*). One of two complementary 30-mer oligonucleotides with the palindromic *pur* gene operator sequence (*21*) was labeled by T4 polynucleotide kinase, using [γ-^{32}P]ATP. The complementary oligonucleotides were then annealed (*21*). PurR−DNA binding was carried out using buffer system II (described above) or buffer system I (5 mM Hepes, pH 8.0, 50 mM KCl, 1 mM EDTA, 10% glycerol) as previously described (*21*) with the following modifications. The concentration of DNA probe was decreased by 200-fold to 2.5 pM, and bovine serum albumin (BSA) was added at a concentration of 50 μg/mL (*24*). PurR was added in concentrations from 1.1 pM to 37.5 nM monomer in the presence of hypoxanthine, and from 4.6 pM to 150 nM monomer in the absence of hypoxanthine. A 20 μL reaction was incubated at room temperature for 30 min before repressor−operator complexes were separated from free DNA by electrophoresis on a 12% polyacrylamide gel as described (*4*). The gel was dried and counted for radioactivity using a Packard Instant Imager. Operator affinity was determined by fitting the binding data to eq 2 (*25*) using Ultrafit software.

$$Y = [PurR]^n/(K_d n + [PurR]^n) \quad (2)$$

Y is fractional saturation, [PurR] is repressor monomer concentration; K_d is the dissociation constant; and *n* is the Hill coefficient.

Circular Dichroism Experiments. All near-UV CD spectroscopy was performed using a JASCO J600 spectropolarimeter. Spectra were collected at room temperature using a 1.0 cm path length quartz cell. A bandwidth of 1 nm with a scan speed of 20 nm/min was used for measurements. Proteins were dissolved to 1 mg/mL in buffer II in the presence or absence of 60 μM Gua. Samples were incubated at room temperature for at least 5 min before measurement. All buffers used for spectral measurements were filtered through 0.22 μm cellulose acetate membranes (Millipore Corp., Bedfore, MA). Protein samples were centrifuged at 13 000 rpm at 4 °C in a microcentrifuge to remove any particulate material before dilution. Each spectrum was the average of 3−4 scans. The spectrum was then recalculated to standard molar ellipticity units Θ (eq 3) and smoothed using JASCO-600 software (*26*):

$$[\Theta] = \frac{\Theta \times 100 \times M_r}{C \times d} \quad (3)$$

where Θ is the measured ellipticity in degrees, *C* is the protein concentration in milligrams per milliliter, *d* is the path length in centimeters, and M_r is the dimer molecular weight.

RESULTS

In Vivo Function of PurR Mutants. X-ray structures have defined two PurR CBD conformational states: closed in the PurR−corepressor−DNA ternary complex (*6*) and open in the apoprotein (*9*). Residues that might mediate or be important for the allosteric transition between closed and open CBD conformations (Figure 1) were targeted for mutagenesis. We focused on a Glu70−Arg278′ salt bridge and on Trp147. The Glu70−Arg278′ salt bridge links the CBD NH_2-subdomain of one subunit to the CBD COOH-subdomain of the other subunit (*6*) in the closed ligand-bound structure (Figure 2). This salt bridge is not seen in the open ligand-free conformation (Figure 3). X-ray structures of ligand-free and bound forms of PurR indicate that Trp147 is integral to the large structural transition in the corepressor binding pocket resulting from ligand binding (*6*, *9*). Following mutagenesis, PurR function was assayed by measuring the capacity for repression of a *purF-lacZ* reporter. In this system, a single-copy chromosomally integrated *purR* gene is expressed at a level that is similar to that of *purR*$^+$ in wild-type cells (*19*). As shown by the data summarized in Table 1 there was 19-fold repression by wild-type PurR, whereas the E70A and W147A mutant proteins functioned as superrepressors, giving 34−52-fold repression. The R278A replacement in which the Glu70−Arg278′ salt bridge was disrupted did not lead to superrepression, but rather this mutant repressor retained 67% of wild-type function. Thus, the increased repression by the E70A protein was not related to the Glu70 salt bridge with R278.

Arg190 and Asp275 make direct hydrogen bonds with corepressor (*6*), and mutations of these residues decrease corepressor binding affinity and consequently in vivo function (*19*, *21*). An Arg190 or an Asp275 replacement was incorporated into the E70A and W147A superrepressors to examine the dominance relationship between putative global conformational changes resulting from E70A and W147A mutations and local perturbations of corepressor binding. The data in Table 1 show that superrepression by W147A was maintained in the W147A/R190A double mutant. Near wild-type repression was obtained in the E70A/D275A double mutant, in striking contrast to the complete loss of function of the D275A repressor. These results indicate that the putative global change resulting in superrepression is dominant to the local perturbation of corepressor binding.

Three cross-subunit contacts were identified between the DNA binding domain of one subunit and the CBD of the other (*6*). These interactions are between the main-chain CO of Gln113 and the backbone NH of Ala49′, and the NH1 and NH2 of Arg115 with the Oγ and main-chain CO of Ser46′ (Figure 4). Site-directed replacements were constructed to assess the functional importance of these cross-

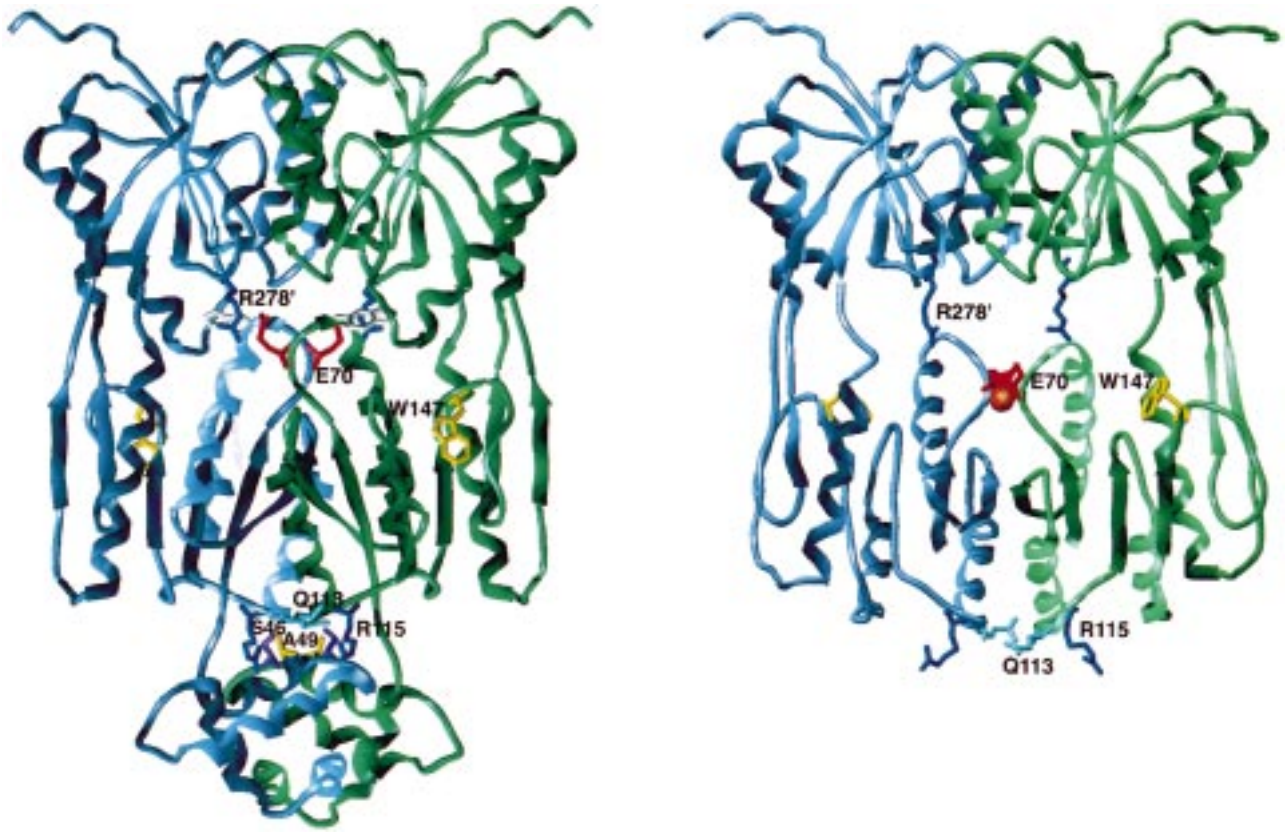

FIGURE 1: Ribbon diagrams of the corepressor-bound or closed (left) and corepressor-free or open (right) conformations of PurR. The structures are presented such that their C-terminal corepressor binding domains (the top domain of each structure) are oriented similarly. One subunit is colored blue and the other green. The side chains of the substituted residues described in this study are displayed as solid sticks, labeled and colored in the following manner: R115 and R278 are blue; E70 is red; W147 is yellow; Q113 is light blue; S46 is purple; and A49 is yellow. The guanine corepressor (not labeled) is shown in white in the closed structure. An orange sphere directly below residues E70 and E70′ indicates the location of a bound magnesium ion in the open conformer (right). The DNA binding domain, containing residues S46 and A49, is not present in the corepressor-free structure.

subunit interdomain hydrogen bonds. R115A and S46G mutations each essentially abolished repressor function (Table 1), thus supporting the importance of these hydrogen bonds. Since a S46A PurR mutant had more than 60% of the wild-type function, the interaction of the Arg115 side chain with the Ser46′ side chain is not critical. Rather, the expected change in backbone ϕ, ψ torsion angles in the S46G mutant (*27*) likely perturbs the Arg115 hydrogen bond to the CO backbone of residue 46′. Therefore, the side-chain−main-chain hydrogen bond and not the side-chain−side-chain hydrogen bond is likely needed for interdomain signaling. On the other hand, Q113G and A49G replacements did not significantly decrease PurR function. These two mutant repressors had essentially wild-type function, suggesting that the Gln113−Ala49′ hydrogen bond either was not disrupted or is not required to transmit the ligand binding signal to the DNA binding domain.

To assess the effect of PurR super repression on *pur* regulon gene expression, the E70A, W147A, and W147A/R190A genes were incorporated into the chromosome of strain R220 (*purR*$^-$ Pur$^+$), and growth rates in minimal medium were determined. Superrepression of the gene encoding the rate-limiting enzyme (presumably *purF*) should limit purine nucleotide synthesis and decrease the growth rate. Data summarized in Table 2 show that the E70A and W147A PurR superrepressors increased the doubling time of the *purR*$^+$ cells by more than 2-fold. As expected, the wild-type PurR had no effect on growth rate (compare *PurR*$^+$ and *purR*$^-$). The PurR R190A mutation, which perturbs corepressor binding affinity and specificity, had a negligible effect on the growth rate of the W147A strain, consistent with the dominant effect of W147A seen in Table 1. Addition of 100 μg/mL adenine to the growth medium restored the wild-type growth rate of all of the mutants (data not shown), thus verifying that the slow growth rate was due to limiting synthesis of purine nucleotides as a result of superrepression.

Purification of Apo-PurR. Genes encoding the wild-type, E70A, W147A, W147A/R190A, R278A, S46G, and R115A repressors were overexpressed (*19*), and the proteins were purified to homogeneity. The expression level and protein elution profile from the two chromatographic columns, DEAE-Sepharose and heparin−agarose, were similar for the wild type and mutants. In contrast to wild-type PurR which was purified in the aporepressor form (*5*, *9*), preliminary X-ray data collection showed that the corepressor was not removed from the W147A superrepressor that was purified by the same procedure (J. L. Huffman and R. G. Brennan, data not shown). Therefore, the superrepressors were further treated by partial denaturation to release the corepressor as described under Materials and Methods. Data from a control experiment showed that [^{14}C]guanine could exchange with the unlabeled bound corepressor after overnight incubation. A gel filtration elution profile for E70A PurR that had been incubated overnight against excess [^{14}C]guanine is shown in Figure 5A. The E70A PurR in fractions 6−10 contained

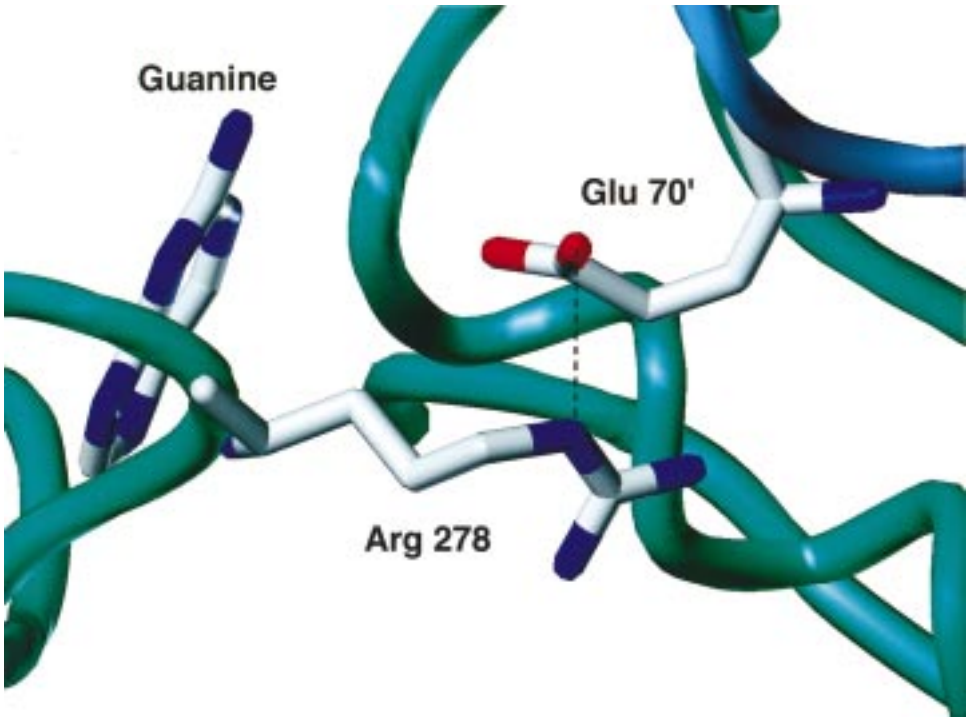

FIGURE 2: Close-up view of the Glu70′−Arg278 ionic interaction in the closed conformation. The side chains are displayed as rounded sticks with nitrogen atoms blue, oxygen atoms red, and carbon atoms white. The trace of the polypeptide backbone of each subunit is shown as a tube, with one subunit in green and the other in blue. The electrostatic interaction is indicated by a black dashed line. A guanine corepressor is included for reference. Hypoxanthine and guanine corepressors give the same closed conformation.

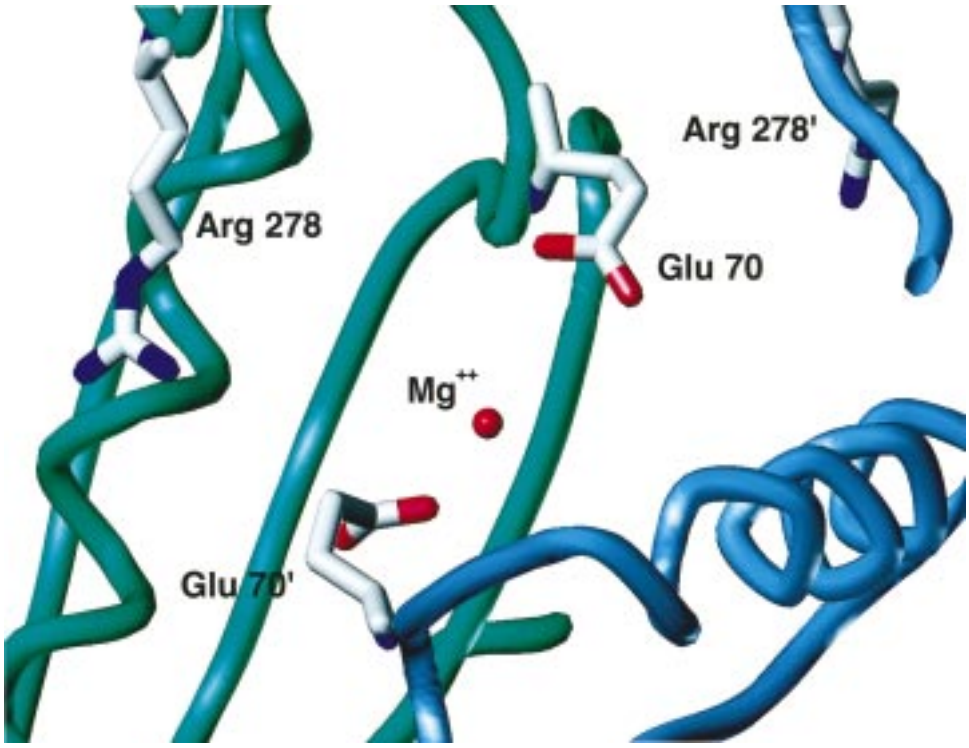

FIGURE 3: Close-up view of the Glu70−Mg^{2+}−Glu70′ interaction in the open conformation. The polypeptide backbones and side chains are colored as in Figure 1. The location of the Arg278 and Arg278′ side chains is shown to emphasize their distance from the Glu70 residues in the corepressor-free conformation.

0.82 equiv of Gua per subunit, whereas fractions 14−24 contained [^{14}C]guanine but no protein. This E70A holorepressor containing [^{14}C]guanine facilitated development of a procedure to remove bound corepressor. The gel filtration profile in Figure 5B shows that radioactive guanine was completely removed by partial denaturation with 1 M guanidinium choloride, column separation, and renaturation. By this procedure, 90% of the E70A PurR was recovered as soluble apoprotein. However, the recovery of the W147A and W147A/R190A repressors was 20%. The remaining protein was insoluble. It was assumed but was not determined directly that the W147A and W147A/R190A super-

Table 1: In Vivo Function of *PurR* Mutants

PurR[a]	β-galactosidase[b] (Miller units)	repression[c] (*x*-fold)
PurR$^-$(vector control)	25.9 ± 1.4	1
PurR$^+$	1.40 ± 0.2	18.5 ± 0.9
E70A	0.50 ± 0.02	51.8 ± 3.5
R278A	2.10 ± 0.5	12.3 ± 2.1
W147A	0.77 ± 0.02	33.6 ± 2.0
R115A	17.4 ± 1.2	1.5 ± 0.2
S46A	2.20 ± 0.4	11.8 ± 2.4
S46G	17.5 ± 1.4	1.5 ± 0.3
Q113G	1.40 ± 0.3	18.5 ± 4.2
A49G	1.60 ± 0.3	16.2 ± 3.1
D275A	32.5[d]	1.2[d]
E70A/D275A	1.80 ± 0.3	14.4 ± 2.2
R190A	3.60 ± 0.6[e]	10.4 ± 0.7[e]
W147A/R190A	0.75 ± 0.03	34.5 ± 3.2

[a] PurR gene or the vector control was integrated into the chromosome of strain FL100 (*purR*$^-$ Δ*lac purF-lacZ*). [b] Values are the average of three independent determinations ± the standard deviation. [c] Repression is calculated as the ratio of β-galactosidase activity from PurR$^-$/PurR (wild type or mutant). [d] Data from (*21*). [e] Data from (*19*).

repressors also contained bound corepressor upon initial purification prior to the partial denaturation procedure.

Binding of Corepressor. Dissociation constants for binding guanine and hypoxanthine to wild-type and PurR mutants were determined by equilibrium dialysis. A representative binding curve for the E70A superrepressor is given in Figure 6. K_d values for guanine and hypoxanthine binding (shown in Table 3) are 0.047 ± 0.002 and 0.33 ± 0.03 μM, respectively. These values reflect a greater than 30-fold higher binding affinity of Gua and Hyp to the E70A superrepressor relative to wild-type PurR. This increased corepressor binding affinity accounts for the presence of bound ligand in the purified superrepressor. The binding stoichiometry was approximately 0.8 equiv ligand per subunit.

E70A aporepressor was used for the experiment shown in Figure 6. However, with E70A holorepressor containing endogenous ligand, binding constants differed by 10% or less, from measurements with aporepressor, consistent with the ligand exchange described above. For this reason, repressor preparations that were not treated to remove endogenous ligand were used for the remaining ligand binding measurements shown in Table 3.

K_d values for Gua and Hyp binding to the W147A superrepressor were decreased by 10-fold relative to wild-type PurR (Table 3). Loss of the Arg190 H bond to the exocyclic O6 of Gua in the R190A repressor increased the K_d for Gua binding by more than 40-fold but as shown in Table 3 had no effect on Gua binding when combined with W147A to make the W147A/R190A double mutant.

K_d values for corepressor binding to the S46G and R115A mutant proteins were unchanged from those of the wild type. Thus, the defective repression by these mutants shown in Table 1 is not due to a perturbation in corepressor binding. Two- to three-fold increased K_ds for corepressor binding to the R278A repressor were detected (Table 3) which could explain the small decrease in repressor function for this mutant shown in Table 1. For all binding determinations shown in Table 3, the Hill coefficients were between 1.5 and 1.7, in close agreement with the value for wild-type PurR obtained previously (*21*). Thus, none of the changes in K_d are due to altered cooperativity.

Binding to Operator DNA. Gel shift assays were carried out to determine the effect of the mutations on repressor−operator DNA interaction. The apparent K_d values are given in Table 3. Wild-type PurR bound operator DNA with a K_d of 3.75 nM, and hypoxanthine corepressor increased the binding affinity by 40-fold (K_d of 0.09 nM). These lower K_d values compared to those reported previously (*5*, *21*) resulted from using a 200-fold lower operator DNA concentration and addition of BSA to stabilize the low concentrations of repressor that were used. For superrepressor mutants, E70A and W147A, the holo- and aporepressor bound to DNA with similar affinity. These results indicate that the E70A and W147A superrepressors assume a closed active conformation in the absence of corepressor. In contrast, the S46G and R115A repressors were essentially disabled for binding to operator DNA. The K_d of holo-S46G for binding was increased over 70-fold compared to the wild-type PurR, and binding of the aporepressor was too weak to detect. Binding of holo- and apo-R115A was too weak for detection. Thus, the corepressor binding signal was not transmitted to the DNA binding domain when the Ser46−Arg115 hydrogen bonds were disrupted. The R278A repressor bound operator DNA similar to the wild type.

A Mg^{2+} ion is observed between the two CBD N-subdomains in the open conformation (PDB code 1DBQ) but not in the closed conformation. Six glutamates (Glu70, Glu79, Glu82 from each subunit) are located within 3.87−5.58 Å of this Mg^{2+}. Thus, Mg^{2+} may stabilize the open conformation by neutralizing the negative charges from some of the six glutamates. To evaluate this possibility, we examined the effect of Mg^{2+} on PurR−operator DNA binding. Apo−PurR exhibits high affinity, corepressor-independent, specific binding to operator DNA in a low ionic strength buffer that does not contain Mg^{2+} (*5*). This buffer has been designated buffer I (*5*). PurR−operator DNA binding was determined in buffer I, with and without added Mg^{2+}, and the binding isotherms are shown in Figure 7. In this buffer with no added Mg^{2+}, apo-PurR bound to operator DNA with a K_d of 0.18 ± 0.03 nM. The K_d was increased by 6.7-fold to 1.20 ± 0.2 nM by 100 mM magnesium acetate. Addition of 50 μM Gua restored the higher affinity binding to operator DNA. DNA binding for PurR mutant E70A did not respond to Mg^{2+} ion under these conditions (data not shown). The results are consistent with a model in which Glu70 side chains from each subunit together with a Mg^{2+} may participate to stabilize the apo-PurR open conformation. Without Glu70, the allosteric equilibrium between open and closed conformations was thus shifted to favor the closed active conformation, even in the absence of corepressor. While other residues may also contribute to stabilizing the open conformation, Glu79 and Glu82 are apparently not involved. An E79A mutant repressor had wild-type function, not superrepression, and an E82A mutant lost repressor function (data not shown). An E70Q PurR gave 9-fold repression; it was not a superrepressor (data not shown).

Circular Dichroism. Changes in protein tertiary structure can be monitored by CD spectra in the near-UV range where the CD signals originate mainly from aromatic amino acids (*28*, *29*). Near-UV CD spectra were obtained to compare the conformational state of wild-type PurR and the E70A and W147A mutants in their corepressor-free and corepressor-bound states (Figure 8). Wild-type PurR with 4 tryp-

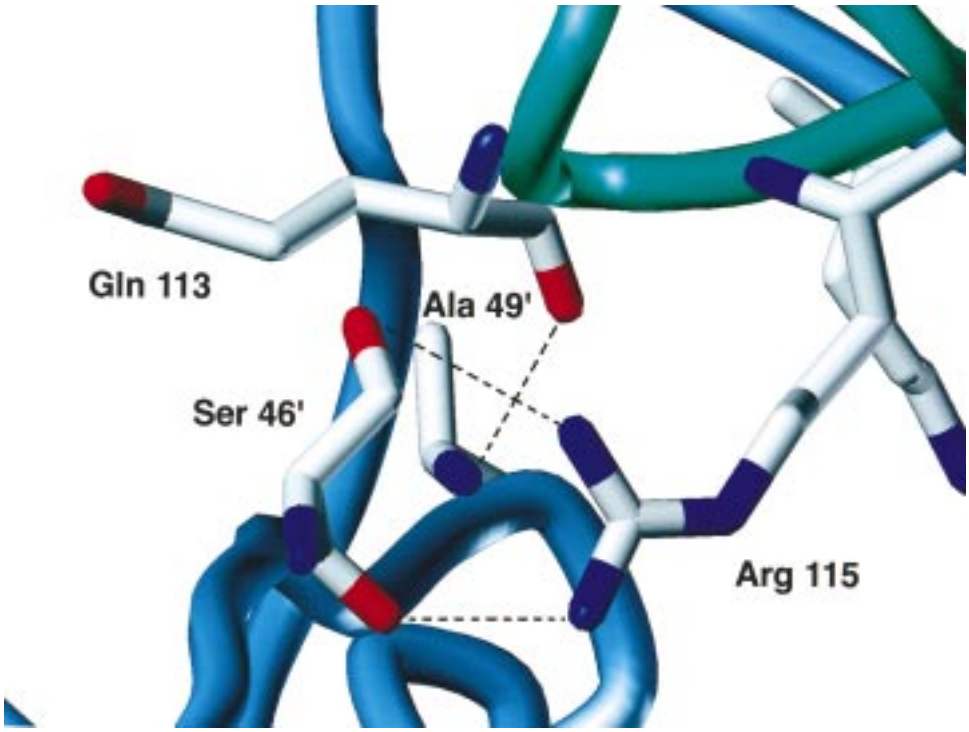

FIGURE 4: Close-up view of the CBD−DNA binding domain interface. The side chains of Ser46 and Ala49, located in the DNA binding domain, and Gln113 and Arg115 in the CBD are displayed as rounded sticks with nitrogen atoms in blue, oxygen atoms in red, and carbon atoms in white. The trace of the polypeptide backbone of each subunit is shown as a tube and colored as in Figure 1. Dashed lines are hydrogen bonds.

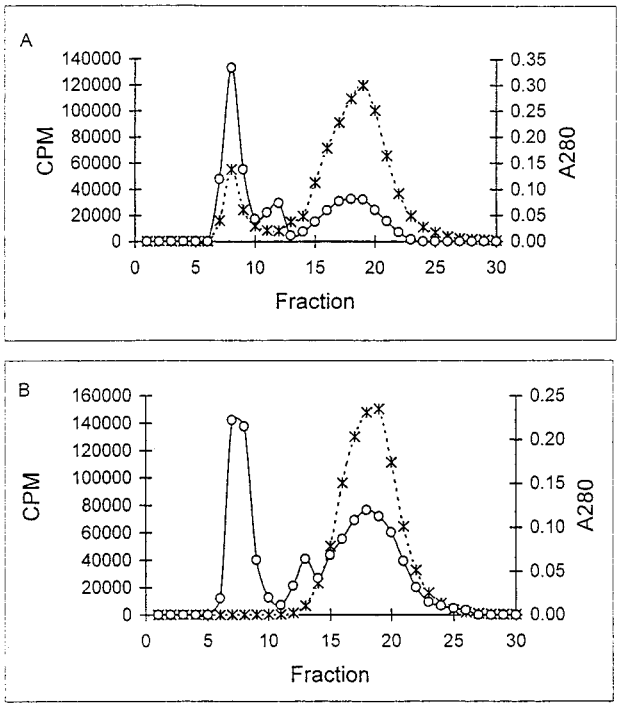

FIGURE 5: Separation of corepressor from the E70A mutant by gel filtration. Radioactivity (×) and absorbance (*A*) at 280 nm (○) are plotted for each fraction. (A) Control experiment in which the protein sample was not treated with 1 M guanidine hydrochloride. Elution was with buffer A. (B) The protein sample was treated with 1 M guanidine hydrochloride, and elution was with buffer A plus 1 M guanidine hydrochloride.

tophan, 12 tyrosine, and 11 phenylalanine residues showed a spectrum with two maxima at approximately 259 and 297 nm and a deep trough with a negative peak at 283 nm. The peak at 259 nm exhibited a shoulder at a wavelength of 263

Table 2: Effect of PurR Superrepressor Mutations on Growth Rate

purR gene[a]	generation time (min)
purR⁻(vector control)	42
purR⁺	42
W147A	90
W147A/R190A	87
E70A	95

[a] PurR genes, or the vector control, were integrated into the chromosome of strain R220 (*purR*⁻). Cells were grown in minimal medium without a purine supplement.

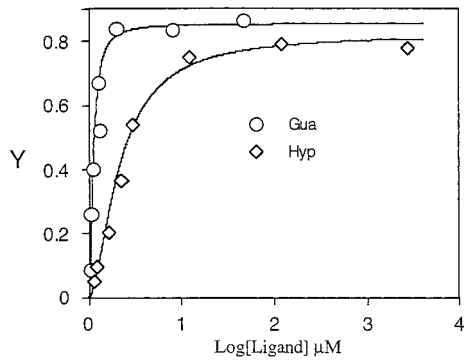

FIGURE 6: Equilibrium binding of corepressors to E70A mutant repressor. The fraction of bound protein (*Y*) is plotted against the free ligand concentration. E70A, monomer aporepressor concentrations of 0.15 and 0.4 μM were used to determine binding of Gua and Hyp, respectively.

nm. Binding of guanine caused a negative enhancement of the near-UV CD signal for the range from 250 to 295 nm, a change of sign for the 259−263 nm region from positive to negative rotation, and increased positive CD from 295 to 310 nm. There was also a small red shift for the 297 nm peak (Figure 8, inset). The enhancement in the CD was

Table 3: Corepressor and Operator DNA Binding by PurR Mutants

repressor	corepressor binding,[a] K_d (μM) Gua	corepressor binding,[a] K_d (μM) Hyp	operator DNA binding,[b] K_d (nM) Hyp	operator DNA binding,[b] K_d (nM) no corepressor
PurR	1.6 ± 0.5[c]	11 ± 1.6[c]	0.09 ± 0.010	3.75 ± 1.12
E70A	0.047 ± 0.002	0.33 ± 0.03	0.12 ± 0.010	0.14 ± 0.018
R278A	5.0 ± 0.8	29 ± 3.8	0.14 ± 0.015	4.55 ± 1.22
W147A	0.16 ± 0.04	0.81 ± 0.04	0.11 ± 0.010	0.15 ± 0.013
S46G	1.8 ± 0.3	11.2 ± 1.3	6.63 ± 2.30	ND[d]
R115A	1.7 ± 0.4	12.0 ± 1.8	ND[d]	ND[d]
R190A	69 ± 10[c]	101 ± 5.5[c]	*e*	*e*
W147A R190A	0.27 ± 0.07	0.64 ± 0.12	*e*	*e*

[a] Dissociation constants were determined by equilibrium dialysis. [b] Operator DNA binding dissociation constants were determined by gel retardation assay in the presence 200 μM hypoxanthine or no corepressor. [c] Corepressor binding data of wild-type and R190A repressors (*19*). [d] Not detected. [e] Not determined.

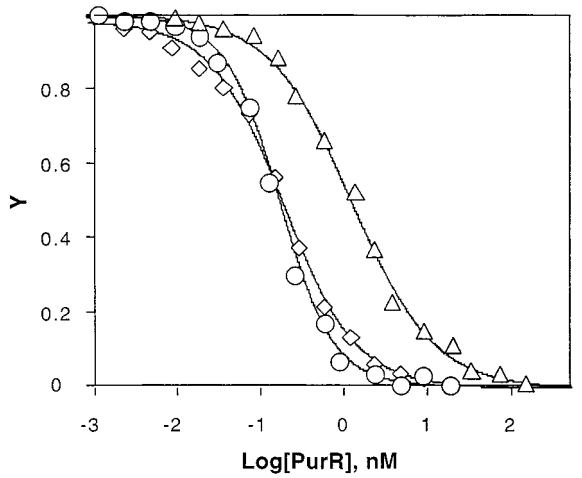

FIGURE 7: Binding isotherms of PurR−operator DNA interaction. The fraction of unbound operator DNA (*Y*) was plotted against the log of PurR monomer concentration. Samples were in buffer I (○), buffer I + 100 mM magnesium acetate (Δ), or buffer I with 100 mM magnesium acetate plus 50 μM Gua (□).

dependent on the guanine concentration until a plateau was reached (data not shown). Although free guanine did not give any near-UV CD signal (data not shown), it is possible that coupling of bound guanine with aromatic side chains could alter the CD bands of side chains or bound purine without a conformation change.

The most significant portion of the CD spectra for comparing the wild-type and mutant repressors was between 297 and 305 nm (Figure 8, insets). Apo forms of wild-type PurR, E70A, and W147A mutant repressors each have a peak of positive ellipticity at 297 nm. Of the aromatic residues, only tryptophan gives a near-UV CD signal in the region from 295 to 305 nm (*29*). The decreased intensity of the 297 nm band in apo-W147A relative to apo-PurR (wild type) is consistent with a portion of this ellipticity in the wild-type originating from Trp147. We interpret the increased intensity of the 297 nm band in apo-E70A repressor as resulting from a conformation that is different from that of the wild-type aporepressor (Figure 8B). Binding of Gua to E70A did not change the CD intensity but red-shifted the maximum by about 1 nm. This indicates that bound guanine does not exhibit $\mu-\mu$ coupling with amino acid side chains in the protein and does not itself contribute to the CD spectrum. It therefore follows that the increased ellipticity seen in Figure 8A (inset) and Figure 8B (inset) for wild-type PurR upon binding Gua must result from a conformation change. Furthermore, E70A repressor has essentially the same closed conformation with or without bound Gua in regions that contribute the 295−305 nm CD whereas Gua binding changes the open PurR wild-type conformation to one more similar to that of E70A which is closed. Binding of Gua also decreased the intensity at 297 nm for W147A. The CD spectrum of holo-W147A differs greatly from that of PurR wild type and E70A repressor because of the absence of Trp147.

To investigate whether corepressor induces a similar conformational change in the CBD of the R115A and S46G mutants as seen for wild-type PurR, we determined the near-UV CD spectra for these two mutant repressors. The spectra for the R115A and S46G apo- and holorepressors were closely similar to those of wild-type PurR in both shape and amplitude (data not shown). Therefore, the CBD in these two mutant repressors undergoes the same open to closed conformational transition upon corepressor binding as in wild-type PurR. However, the structure change in the CBD is not transmitted to the DNA binding domain when the Arg115−Ser46 interaction is disrupted.

DISCUSSION

X-ray structures of a PurR−hypoxanthine−*purF* operator complex (*6*) and a ligand-free PurR CBD dimer (*9*) have defined conformers that bind operator DNA with high and low affinity, respectively. From these structures, an allosteric mechanism was suggested to explain how corepressor mediates specific binding to DNA (*9*). According to the current model, binding of corepressor at the interface of the two CBD subdomains results in structural changes that include hinge bending rotations of 17° and 23° between the NH_2- and COOH-subdomains of each monomer and convert an open CBD conformation to a closed one. It was deduced that these rotations position DNA binding domain hinge residues 48−56 of each subunit in closer proximity to each other so that in the presence of operator DNA, helices form and interact with the DNA minor groove. This minor groove interaction kinks the operator site by greater than 46°, thus enabling base-specific contacts of the 2-fold related helix−turn−helix motifs with the DNA major grooves. We assume that there is an equilibrium between the active DNA binding structure having the closed CBD conformation, in which the DNA binding domains are poised for binding, and the structure in the open conformation that should be incapable of binding to DNA. In the absence of corepressor, this equilibrium must strongly favor the inactive open conformation. Binding of corepressor results in a shift of the equilibrium to the active DNA binding closed conformation. The equilibrium between the open and closed conformations can be assumed to be influenced by amino acid side chain and backbone interactions that stabilize or destabilize one or the other of the conformations. In this study, we have mutagenized residues noted previously (*6*, *9*) to make prominent interactions that may be important for the active or inactive conformations.

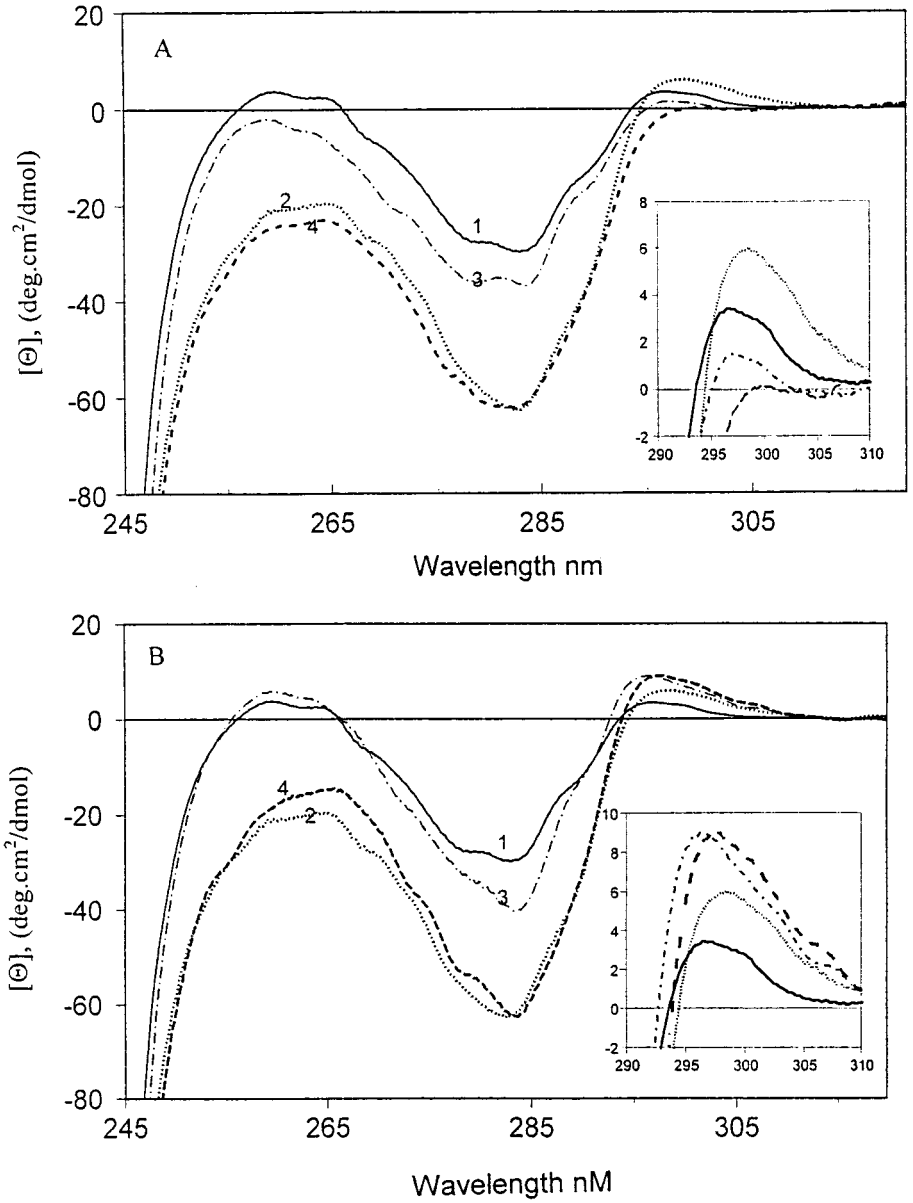

FIGURE 8: Near-UV CD spectra of wild-type and mutant PurR in the presence or absence of 60 μM Gua. The protein concentration was 1 mg/mL in buffer II. (A) Spectra of wild type and W147A mutant. The spectra are for (1) wild type, (2) wild type + Gua, (3) W147A, (4) W147A + Gua. (B) Spectra of wild-type and E70A mutant. The spectra are for (1) wild type, (2) wild type + Gua, (3) E70A, and (4) E70A + Gua. The insets show an expanded view of the 290−310 nm region.

Trp147 and Glu70 Are Involved in the CBD Allosteric Transition. Two residues, Glu70 and Trp147, were shown to have important roles in the allosteric transition. Three lines of evidence indicate that the allosteric equilibrium has been perturbed and the E70A aporepressor and the W147A aporepressor are largely in the active closed conformation. First, these aporepressors bind to the *pur* gene control site with a K_d that is similar to that of wild-type holo-PurR. These mutant repressors exhibit high-affinity DNA binding in the absence of corepressor. Whereas corepressor binding increased the affinity of wild-type PurR for the operator DNA site by over 40-fold, there was essentially no further activation of the E70A and W147A repressors by corepressor. Second, binding affinities of corepressors for the mutant repressors were increased 30-fold for E70A and 10−13-fold for W147A relative to the wild type. Since there were no mutational changes in the corepressor binding pocket of the E70A repressor, and no changes in the Trp147 mutant of any residue directly contacting the bound repressor, the increased corepressor binding affinity is ascribed to a higher equilibrium concentration of closed conformer. Even the R190A replacement, which alters important hydrogen bonding interactions with bound corepressor (*19*) and decreases the binding affinity for guanine by 40-fold, only marginally decreased the guanine binding affinity when it was combined into the W147A repressor. The CD conformational probe provided the third line of evidence that the apo-E70A CBD was in a closed conformation. A peak of positive rotation at 297 nm that reflects the conformation of the corepressor binding pocket was used to monitor the transition from open to closed CBD upon binding corepressor. The intensity of this peak in apo-E70A corresponds to that of the closed conformation and was not further increased upon binding of guanine. CD thus provides strong evidence that the allosteric equilibrium for apo-E70A repressor is largely shifted to the active, closed

conformation and does not undergo a further change upon binding guanine.

The functional consequence of these mutations that shift the allosteric equilibrium was to create repressors that down-regulate *purF* expression 2−3-fold more than wild-type PurR. This superrepression inhibited the cell growth rate by starving cells for purines.

The thermodynamic basis for the shift in allosteric equilibrium in the two Trp replacements is likely a destabilization of the open conformation. In ligand-free CBD, the indole moiety of Trp147 rotates into the corepressor binding pocket and stacks against Tyr73 and Phe74 and its Nϵ forms a hydrogen bond to the side chain of Tyr73. In this way Trp147 acts as a structural, but not a functional, surrogate for corepressor. To form the closed state, hypoxanthine or guanine displaces Trp147 from the purine binding pocket. The displacement of Trp147 and its nearby region leads directly to disruption of a hydrogen bond between the side chains of Asp160 and Asn161. The loss of this hydrogen bond is correlated with a change in ψ, ϕ torsion angles of residues Asp160 and Asn161 located in the hinge between the COOH- and NH_2-subdomains, which is responsible in great part for the hinge bending rotations of 17° and 23° between the NH_2- and COOH-subdomains.

The stereochemical basis of the shift in the allosteric equilibrium of the E70A superrepressor to the closed conformation is not clear. In the closed conformation, Glu70 makes a salt bridge to Arg278 of the other subunit. However, this interdomain salt bridge is not important for stabilizing the closed conformation since an R278A replacement had only a minimal effect on corepressor binding affinity and repressor function. In the open conformation, Glu70 is repositioned such that it occupies a solvent-exposed area at the interfaces of the CBD subdomains. This region is electrostatically negative because of the proximity of acidic residues, Glu79, Glu82, and their dyadic mates as well as Glu70 and Glu70′. To mitigate partially the negative potential, a Mg^{2+} ion binds in this area and interacts primarily with Glu70 and Glu70′. That such an interaction stabilizes the open conformation is suggested by the finding that added Mg^{2+} ion decreased PurR−DNA affinity but had no effect on apo-E70A−DNA binding. Further evidence that supports the critical need for a negative charge at position 70 and not position 79 or 82 is provided by the neutralized mutant, E70Q, which although isosteric results in some loss of repressor function, and E79A and E82A, which display wild-type and loss of function properties, respectively, rather than act as superrepressors. Therefore, the role of Glu70, its 2-fold mate, and the Mg^{2+} ion appears to be that of an electrostatic wedge, which through the combination of electrostatic attraction and repulsion maintains the proper orientation and distance between the CBD NH_2-subdomains necessary to stabilize the NH_2-subdomain interface of the aporepressor.

Although Glu70 and Trp147 mutations were shown to perturb the PurR allosteric equilibrium, this does not exclude the possibility for participation of additional amino acids. It is in fact likely that a number of key interactions contribute to stabilization of the open and closed conformations. In aspartate transcarbamoylase, at least four residues have roles to stabilize the inactive conformation, and four residues were identified for stabilizing the active conformation (*11*). Recently, Ala110 was reported to influence the allosteric equilibrium between DNA binding and inducer binding conformations of Lac repressor (*30*). It was suggested that an A110T mutation stabilized the inducer binding conformation, thus shifting the equilibrium toward the state having an increased affinity for IPTG. An A110K mutation, on the other hand, was thought to stabilize the DNA binding conformation, thus giving high-affinity DNA binding due to the increased relative amount of this form. Interestingly, the side chain of the corresponding PurR residue, Tyr107, makes an intersubunit hydrogen bond to the backbone CO of Tyr90′ in the open conformation, while in the closed conformation, this residue is relocated to stack against Phe86′ and hydrogen bond to Glu82′. Given these alternative sets of stabilizing interactions, it is possible that Tyr107 is involved similarly in the allosteric equilibrium of PurR. Mutations at a single position that displace the allosteric equilibrium of PurR toward each of the opposing conformers have not been isolated to date.

Interdomain Signaling. Three hydrogen bonds provide connections between the CBD and the DNA binding domain in the closed state. These interdomain, intersubunit hydrogen bonds are between the NH1 and NH2 of Arg115 and the side-chain Oγ and main-chain CO of Ser46′, and the main-chain CO of Gln113 with the backbone NH of Ala49′. Our mutational analysis has provided evidence for an important role for the Arg115 side-chain−Ser46′ backbone interaction as truncation of the R115 side chain to alanine strongly disabled repressor function. In contrast, removal of the hydroxyl group of Ser46 (S46A) results in a repressor which retained about 60% of wild-type function, indicating the lesser importance of the weaker Arg115 NH1−Ser46′ Oγ hydrogen bond (3.5 Å) compared to the hydrogen bond (3.0 Å) between the main-chain carbonyl oxygen of Ser46′ and NH2 of Arg115 in interdomain signaling. However, further truncation of the Ser46 side chain to glycine disrupted repressor function completely. Presumably, the underlying structural basis for this nonfunctional repressor is the inability of a glycine residue at position 46 to assume the dihedral angles necessary to form the wild-type main-chain hydrogen bond to Arg115 of the other subunit, despite the ability of R115A and S46G to bind corepressor with virtually wild-type affinity and to undergo the CBD structural change that is detected by CD. Thus, it appears that the loss of this single interaction disrupts in toto the interdomain signal of corepressor binding.

Mutations designed to disrupt Gln113−Ala49 had no effect on repressor function. It is not known whether these mutations disrupted the main-chain to main-chain hydrogen bond as was intended or if the hydrogen bond is not required for signaling. From our analysis, it appears that residue Ser46, which is located in the middle of a five-residue loop, is pivotal in tethering helix 3 and the helix−turn−helix motif to the hinge helix and CBD. Thus, the critical role of the hydrogen bond between Arg115 and Ser46′ for signal transmission may be determined by both the strong interaction and the position of the hydrogen bond.

To our knowledge this is the first of the bacterial repressors having distinct DNA binding and effector binding domains in which interdomain signaling residues were functionally and structurally identified. It remains to be determined if other Lac family repressors employ a similar signal transmission mechanism.

ACKNOWLEDGMENT

We thank Joy L. Huffman for help in preparation of figures showing structural features of PurR.

REFERENCES

1. Zalkin, H., and Nygaard, P. (1996) Biosynthesis of purine nucleotides. in *Escherichia coli and Salmonella, cellular and molecular biology* (Neidhardt, F. C., Curtiss, R., III, Ingraham, J. L., Lin, E. C. C., Low, K. B., Magasanik, B., Reznikoff, W. S., Riley, M., Schaechter, and Umbarger, H. E., Eds.) pp 561−579, American Society for Microbiology, Washington, DC.
2. Rolfes, R. J., and Zalkin, H. (1988) *Escherichia coli* gene *purR* encoding a repressor protein for purine nucleotide synthesis. Cloning, nucleotide sequence, and interaction with *purF* operator. *J. Biol. Chem. 263*, 19653−19661.
3. Choi, K. Y., and Zalkin, H. (1992) Structural characterization and corepressor binding of the *Escherichia coli* purine repressor. *J. Bacteriol. 174*, 6207−6214.
4. Choi, K. Y., and Zalkin, H. (1994) Role of the purine hinge sequence in repressor function. *J. Bacteriol. 174*, 1767−1772.
5. Rolfes, R. J., and Zalkin, H. (1990) Purification of the *Escherichia coli* purine regulon repressor and identification of corepressors. *J. Bacteriol. 172*, 5637−5642.
6. Schumacher, M. A., Choi, K. Y., Zalkin, H., and Brennan, R. G. (1994) Crystal structure of LacI member, PurR bound to DNA: minor groove binding by α helices. *Science 266*, 763−770.
7. Weickert, M., and Adhya, S. (1992) A family of bacterial regulators homologous to Gal and Lac repressors. *J. Biol. Chem. 267*, 15869−15874.
8. Nguyen, C. C., and Saier, M. H., Jr. (1995) Phylogenetic, structural and functional analysis of the LacI−GalR family of bacterial transcription factors. *FEBS Lett. 377*, 98−102.
9. Schumacher, M. A., Choi, K. Y., Lu, F., Zalkin, H., and Brennan, R. G. (1995) Mechanism of corepressor mediated specific DNA binding by purine repressor. *Cell 84*, 147−155.
10. Perutz, M. F. (1979) Regulation of oxygen affinity of hemoglobin. *Annu. Rev. Biochem. 48*, 327−386.
11. Kantrowitz, E. R., and Lipscomb W. N. (1988) *Escherichia coli* aspartate transcarbamoylase: the relation between structure and function. *Science 241*, 668−674.
12. Ladjimi, M. M., and Kantrowitz, E. R. (1988) A possible model for the concerted allosteric transition in *Escherichia coli* aspartate transcarbamoylase as deduced from site-directed mutagenesis studies. *Biochemistry 27*, 276−283.
13. Schirmer, T., and Evans, P. R. (1990) Structural basis of the allosteric behavior of phosphofructokinase. *Nature 343*, 140−145.
14. Otwinowski, Z., Schevitz, R. W., Zhang, R. G., Lawson, C. L., Joachimiak, A., Marmonstein, R. Q., Luisi, B. F., and Sigler, P. B. (1988) Crystal structure of trp repressor/operator complex at atomic resolution. *Nature 334*, 321−329.
15. Rafferty, J. B., Somers, W. S., Saint-Girons, I., and Philipps, S. E. V. (1989) Three-dimensional crystal structure of *Escherichia coli* met repressor with and without corepressor. *Nature 341*, 705−710.
16. Somers, W. S., and Phillips, S. E. V. (1992) Crystal structure of the Met repressor−operator complex at 2.8 Å resolution reveals DNA binding by β-strands. *Nature 359*, 387−393.
17. Nagadoi, A., Morikawa, S., Nakamura, H., Enari, M., Kobayashi, K., Yamamoto, H., Sampei, G., Mizobuchi, K., Schumacher, M. A., Brennan, R. G., and Nishimura, Y. (1995) Structural comparison of the free and DNA bound forms of the purine repressor DNA binding domain. *Structure 3*, 1217−1224.
18. Kunkel, T. A., Roberts, J. D., and Zakour, R. A. (1987) Rapid and efficient site-directed mutagenesis without phenotype selection. *Methods Enzymol. 154*, 367−382.
19. Lu, F., Schumacher, M. A., Arvidson, D. N., Haldiman, A., Wanner, B. L., Zalkin, H., and Brennan, R. G. (1998) Structure-based redesign of corepressor specificity of the *Escherichia coli* purine repressor by substitution of residue 190. *Biochemistry 37*, 971−982.
20. Layne, E. (1957) Spectroscopic and turbidometric methods for measuring protein. *Methods Enzymol. 3*, 447−454.
21. Choi, K. Y., Lu, F., and Zalkin, H. (1994) Mutagenesis of amino acid residues required for binding of corepressors to the purine repressor. *J. Biol. Chem. 269*, 24066−24072.
22. Miller, J. H. (1992) *Experiments in molecular genetics*, Cold Spring Harbor Laboratory, Cold Spring Harbor, NY.
23. Rolfes, R. J., and Zalkin, H. (1988) Regulation of *Escherichia coli purF*. Mutations that define the promoter, operator, and purine repressor gene. *J. Biol. Chem. 263*, 19649−19652.
24. Xu, H., Moraitis, M., Reedstrom, R. J., and Matthews, K. S. (1998) Kinetics and thermodynamic studies of Purine repressor binding to corepressor and operator DNA. *J. Biol. Chem. 273*, 8958−8964.
25. Liu, Y. C., and Matthews, K. S. (1993) Dependence of *trp* repressor-operator affinity, stoichiometry, and apparent cooperativity on DNA sequence and size. *J. Biol. Chem. 268*, 23239−23249.
26. Schmid, F. X. (1989) Spectral methods of characterizing protein conformation and conformational changes. in *Protein Structure, a practical approach* (Creighton, T. E., Ed.) pp 251−283, IRL Press at Oxford University Press, Oxford, England.
27. Ramachandran, G. N., and Sasisekhan, V. (1968) Conformation of polypeptide and proteins. *Adv. Protein Chem. 23*, 283−248.
28. Strickland, E. H., Horwitz, J., and Billups, C. (1969) Fine structure in the near-UV CD and absorption spectra of tryptophan derivatives and chymotrypsinogen A at 77 K. *Biochemistry 8*, 3205−3211.
29. Strickland, E. H. (1974) Aromatic contributions to circular dichroism spectra of proteins. *CRC Crit. Rev. Biochem. 2*, 113−175.
30. Müller-Hartman, H., and Müller-Hill, B. (1996) The side-chain of the amino acid residue in position 110 of the lac repressor influences its allosteric equilibrium. *J. Mol. Biol. 257*, 473−478.

BI981617K